












RESEARCH ARTICLE | JULY 31 2023

Design, fabrication, and characterization of picowell arrays on cyclic olefin copolymer surfaces generated with a 10.5 MeV N⁴⁺ ion microbeam **FREE**

I. Bányász ; I. Rajta ; V. Havránek ; A. Mackova ; A. J. Laki ; M. S. Z. Kellermayer ; Z. Szittner ; S. Kurunczi ; Sz. Novák ; I. Székács ; R. Horváth ; M. Fried ; G. U. L. Nagy



Appl. Phys. Lett. 123, 053701 (2023)

<https://doi.org/10.1063/5.0155681>



View
Online



Export
Citation

CrossMark

500 kHz or 8.5 GHz?
And all the ranges in between.

Lock-in Amplifiers for your periodic signal measurements



Find out more

 Zurich
Instruments

Design, fabrication, and characterization of picowell arrays on cyclic olefin copolymer surfaces generated with a 10.5 MeV N⁴⁺ ion microbeam

Cite as: Appl. Phys. Lett. **123**, 053701 (2023); doi: 10.1063/5.0155681

Submitted: 22 April 2023 · Accepted: 15 July 2023 ·

Published Online: 31 July 2023



View Online



Export Citation



CrossMark

I. Bányász,^{1,a)} I. Rajta,² V. Havránek,³ A. Mackova,^{3,4} A. J. Laki,^{5,6} M. S. Z. Kellermayer,⁶ Z. Szttnér,⁷ S. Kurunczi,⁷ Sz. Novák,⁷ I. Székács,⁷ R. Horváth,⁷ M. Fried,^{8,9} and G. U. L. Nagy²

AFFILIATIONS

¹Wigner Research Centre for Physics, P.O. Box 49, H-1525 Budapest, Hungary

²Atomki, Institute for Nuclear Research, P.O. Box 51, H-4001 Debrecen, Hungary

³Nuclear Physics Institute AV CR, 250 68 Řež near Prague, Prague, Czech Republic

⁴Department of Physics, Faculty of Science, J. E. Purkinje University, Pasteurova 3544/1, 400 96 Ústí nad Labem, Czech Republic

⁵Faculty of Information Technology and Bionics, Pázmány Péter Catholic University, Práter u. 50a, H-1083 Budapest, Hungary

⁶Department of Biophysics and Radiation Biology, Semmelweis University, Tűzoltó u. 37-47, H-1094 Budapest, Hungary

⁷Nanobiosensorics Laboratory, Centre for Energy Research, Konkoly-Thege Rd. 29-33, H-1121 Budapest, Hungary

⁸Centre for Energy Research, Konkoly-Thege Rd. 29-33, 1121 Budapest, Hungary

⁹Institute of Microelectronics and Technology, Óbuda University, P.O. Box 112, Budapest 1431, Hungary

^{a)} Author to whom correspondence should be addressed: banyasz.istvan@wigner.hu

ABSTRACT

Handling of picoliter-to-nanoliter-scale volumes and objects has increasing importance in life sciences. This is the volume scale of cell extractions and individual living cells. Here, we introduce a method of generating a picoliter-scale device by direct writing of picowell arrays on a ZEONORTM copolymer surface with high-energy medium-mass ion microbeam. Arrays of various microstructures were written in the sample using a microbeam of 10.5 MeV N⁴⁺ ions at various implanted ion fluences. The best array was obtained by implantation of annuli of 10 and 11 μm of inner and outer diameters with a fluence of 7.8×10^{12} ions/cm².

Published under an exclusive license by AIP Publishing. <https://doi.org/10.1063/5.0155681>

An array of 9×9 picowells, in the form of chalice-like structure, was obtained and tested. The implanted surface structures were studied by optical and atomic force microscopy (AFM). The average volume of the picowells was 820 femtoliter (fl), ideal to host a single living cell. AFM microhardness measurements showed that the implanted toroidal wall of the picowell had the same hardness as the unimplanted parts of the sample. Applicability of the ion microbeam written picowell array in biomedical single-cell assays was demonstrated by placing individual cancer cells with the cell-cycle reporter fluorescent construct in some of the wells and detecting their fluorescence signal.

Microplates, consisting of multiple wells, are standard tools in analytical research and clinical diagnostic testing.¹ The earliest

microplate was created in 1951 by Takátsy, who machined six rows of 12 wells in Lucite.² Nowadays, the volume of an individual well on a microplate typically varies between tens of nanoliters to several milliliters.

In modern biochemical assays, there is a need for decreasing individual microwell volume; hence, the need for increasing microwell density arises. Nanowell arrays are nowadays quite common.^{3,4} Fabrication of even smaller microrecipients in the picoliter or even femtoliter range is challenging.^{5–10} An example of a commercial picowell plate product is a 5×12 array of a volume of 28 pl.¹¹ Spatial arraying allows for the characterization and identification of single cells based on genetic profiling,^{12–14} cytokine expression,^{15,16} antibody production,^{17–19} and most recently proteomics.²⁰ The potential of

applying and activating single cells in separate wells, allows for high-throughput analysis of multiple targets simultaneously. Smaller cell culture volumes may provide more concentrated supernatants, improving detection limits and sample recovery rates as well.²¹

Cyclo-olefin copolymers (COC) have excellent optical properties, biocompatibility, and inertness,^{22,23} making them well-suited for bio-marker detection in various biological fluids.²⁴ COCs are becoming more and more popular in generating microdevice and microfluidic substrates.^{25–27} Compared to polydimethylsiloxane (PDMS), a commonly used support material, COCs demonstrate longer shelf life and improved stability. Moreover, the functionalization of COC and its applications have been demonstrated in immunoassays²⁴ and DNA hybridization.²⁸ Nowadays, COCs are considered excellent starting polymers to produce next-generation optical biosensors.^{29–31} Functionalization of ZEONOR™ (Zeon, ZEONOR) has been demonstrated with DNA,³² protein probes,²⁷ and nanoparticles.³³ Efforts have also been made to reduce nonspecific binding with ZEONOR™-based sensors and microdevices.³⁴

Fabrication of optical, microfluidic, and other elements and devices in polymers is a broad and dynamic research field.^{35–44} A critical review on nanomanufacturing of biopolymers using electron and ion beams was written by Jiang *et al.*⁴⁵ However, effects of ion beam implantation on the target material depend on various factors, including the material composition, ion species, energy, implanted fluence, and current density during implantation. The surface structure is governed by different, competing physical and/or chemical processes (such as chain scissioning and cross-linking in polymers) on the microscopic level. In polydimethylsiloxane (PDMS), for instance, compaction has been observed over a wide range of ion fluence when irradiated with both light³⁹ and medium-heavy ions.⁴⁰ However, in polytetrafluoroethylene (PTFE), the surface topography change depends not only on the delivered ion fluence,⁴³ but also on the current density of the irradiating beam.⁴⁶ In general, in the lack of knowledge of the exact physical and chemical processes for a given system, it cannot be determined *a priori* whether an implantation results in swelling or compaction of the implanted area of the polymer target. Likewise, one cannot always predict the distribution of refractive index change induced in the material.

While COC microchannels have the potential to improve both the optical detection sensitivity and the chemical resistance of polymer microanalytical systems, their surface properties have not been

characterized thoroughly so far. These surface properties play a crucial role in various aspects, including electrokinetic effects in the presence of electric fields. Although the source of the surface charge remains unclear, chemical functionalization studies have indicated the absence of carboxylic acid groups on the surface, which is consistent with the chemical structure of ZEONOR™.⁴⁷ The main characteristics of this material are excellent: less than 0.01% water absorption per 24 h, 92% optical transmission in the 400–800 nm range, small specific gravity of 1.01 g/cm³, glass transition range of 100–130 °C, melt flow rate of 20–60 g/10 min, high chemical resistance, and low permeability.⁴⁸

In view of our previous results regarding ion beam implantation of optical and mechanical elements in polymers, we designed two types of implanted patterns: a homogeneously implanted disk and a homogeneously implanted annulus. In focused ion beam lithography, low-energy ion (1–50 keV) is used, which creates microstructures on the surface by sputtering.^{45,49} We used a microbeam of a high-energy medium-mass ion for the fabrication of the picowell arrays, exploiting the chain scissioning and cross-linking processes; hence, producing compaction or swelling of the material.

Some recent experience was also obtained in the use of such ion beams for the fabrication of microstructures in polymers.^{50–53} Romanenko *et al.* reported surface relief structures of an amplitude of 900 nm using a microbeam of 2 MeV He²⁺ ions at a fluence of 1.6×10^{14} ions/cm². They also achieved an amplitude of 2 μm by a microbeam of 10 MeV O⁴⁺ ions at a fluence of 8×10^{13} ion/cm² in a pure PDMS sample.⁵¹

Irradiations were conducted at the 3 MV Tandatron 4130 MC accelerator (High Voltage Engineering Europa B.V.) of the Řež Nuclear Physics Institute, Czech Republic.⁵⁴ A microbeam of 10.5 MeV N⁴⁺ ions was used for direct writing of the structures. The beam size was $3 \times 3 \mu\text{m}^2$, the current was 800 pA, resulting in a beam current density of 88.9 A/m². Ten arrays of microstructures were irradiated, the parameters of these arrays are presented in Table I.

The Stopping and Range of Ions in Matter (SRIM) code⁵⁵ was used to calculate the electronic and nuclear stopping power. Electronic stopping power was 98 eV/Å at the sample surface, and it reached a broad peak of 104 eV/Å at 4.5 μm below the surface. It decreased to half of the maximum at a depth of 10.4 μm. Nuclear stopping power had a sharp Bragg peak of 3 eV/Å at a depth of 12.8 μm. The electronic interaction was clearly dominant. This is presumably responsible for the surface structure formation, since molecular re-arrangement due

TABLE I. Parameters of the ion microbeam-written microstructures.

Array name	Irradiation pattern	r_1 (μm)	r_2 (μm)	Spacing between individual wells (μm)	Fluence (10^{12} ions/cm ²)
A	Disk	5	...	15	100
B	Disk	5	...	15	15.6
C	Disk	5	...	15	15.6
D	Disk	5	...	15	7.8
E	Disk	5	...	30	7.8
F	Disk	5	...	30	15.6
G	Disk	5	...	30	>15.6
H	Annulus	3	4	50	7.8
I	Annulus	3	4	50	7.8
J	Annulus	10	11	50	7.8

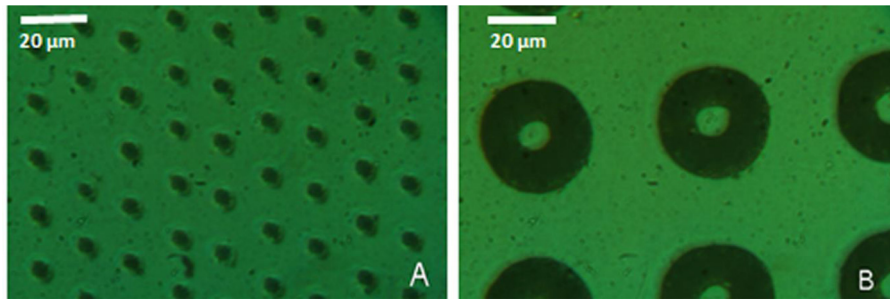


FIG. 1. INTERPHAKO microphotos of ion microbeam irradiated microstructures in ZEONOR™. (a) Part of array D, disk-irradiated elements. Diameter of the irradiated disks is $5\ \mu\text{m}$. (b) Part of array J, ring-irradiated elements. Outer diameter of the irradiated rings is $22\ \mu\text{m}$. Zeiss Peraval microscope, $63\times$ objective, $63\times$ ring aperture, green interference filter for both microphotos.

to bond-breaking and bond-formation in polymers upon ion irradiation is effectively induced by electronic interactions with the ion beam.^{56,57}

It was found that the ion microbeam implanted structures could hardly or not at all be detected by conventional transmission microscopy. In other words, they were phase objects, that is the ion beam implantation caused variations mainly in the surface topography and in the index of refraction of the sample. Consequently, the structures were studied by a Zeiss Peraval optical transmission microscope in the INTERPHAKO mode.⁵⁸ That technique, along with interference- and phase contrast microscopy, transforms optical path variations across the object into absorption variations. INTERPHAKO microphotos of two structures are shown in Figs. 1(a) and 1(b). The first one was produced by homogeneously irradiating a disk-shaped area, while the second by homogeneously irradiating a ring-shaped area. It must be noted that white light illumination results in the appearance of interference colors in the microscopic image. The microphotos presented in Fig. 1 were recorded by using a green interference filter. This technique shows the integral of the optical path variations through the sample, i.e., changes both in the surface relief and in the index-of-refraction. Thus, profilometry is required to determine the surface map of the irradiated structures, for which we employed AFM.

The topographical structure of the samples was investigated using a Nanosurf Easyscan 2 AFM instrument in air, with a ContAI-G cantilever. No elastic modulus was observed using atomic force spectroscopy. AFM image of part of array D and the topographical height profile of one of its elements are presented in Fig. 2. It is clearly shown that irradiation of a disk area produced a lens-like swelling at a height of $700\ \text{nm}$. Consequently, no picowell was formed by irradiating that pattern.

AFM image of part of array J and the topographical height profile of one of its elements are presented in Fig. 3. Irradiation of a ring-shaped area resulted in the formation of a chalice bounded by a torus of

a height of $4700\ \text{nm}$. The height of the lens-like structure shown in Fig. 2 is much smaller than that of the torus shown in Fig. 3, in spite of having received the same fluence of 7.8×10^{12} ions/cm². This can be attributed to the fact that, due to the elasticity of the sample surface, it is much easier to inflate the surface on a narrow ring than on a large disk.

The torus encloses a truncated cone-shaped volume. The lower diameter of the truncated cone is about $5\ \mu\text{m}$, whereas the upper one is about $10\ \mu\text{m}$. The height of the picowell was calculated as the average of the three profiles in Fig. 3(b). The average volume of picowells in the array was $820 \pm 65\ \text{fl}$. This volume is much smaller than those of the individual wells of the majority of commercially available picowell arrays. Although in this work, we demonstrated only one effective chip, it is important to note that the direct-write nature of the proposed fabrication method enables the simple re-design of the pattern, allowing for easily modifying the geometry or the array size. In addition, the use of a different beam (mass, energy, or spot size) also opens the possibility to fine-tune the exact shape of the picowells in the array.

It must also be stated that the depth of the implanted picowells depends not only on the implanted ion fluence but also on the current density of the implanting ion microbeam. We have performed the implantation of picowells using the same fluences, but the beam current of the $10.5\ \text{MeV N}^{4+}$ ion beam was only $16\ \text{pA}$ in the first additional experiment, and $125\ \text{pA}$ in the second one. Microbeam sizes were slightly varying between $2.5 \times 2.5\ \mu\text{m}^2$ and $3 \times 3\ \mu\text{m}^2$.

The present experiments performed with a microbeam of a current of $800\ \text{pA}$ and a current density of $88.9\ \text{A/m}^2$ resulted in picowells of an average depth of $4.7\ \mu\text{m}$. The $125\ \text{pA}$ microbeam of a current density of $20\ \text{A/m}^2$ produced a maximum of $400\ \text{nm}$ of picowell depth. Picowells of a maximum depth of $50\ \text{nm}$ were obtained with the microbeam of a current of $16\ \text{pA}$ and a current density of $2.19\ \text{A/m}^2$.

To check mechanical stability of the picowells, nanoindentation was performed both on an irradiated torus and on an unirradiated part of the sample. This way the microhardness in both the irradiated

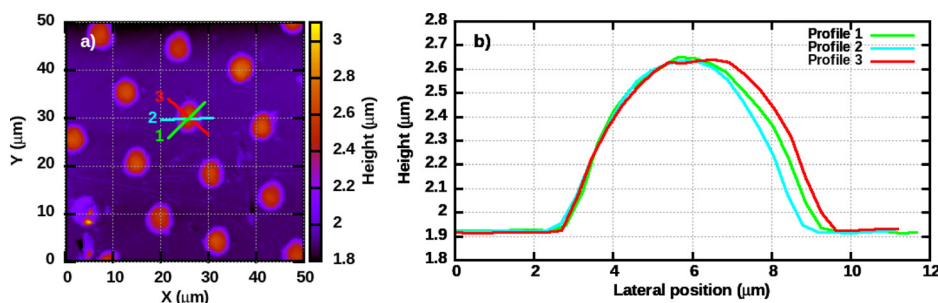


FIG. 2. Height-contrast AFM image (a) of part of array D, and topographical height profiles along the indicated sections of a user-defined single element (b) in it.

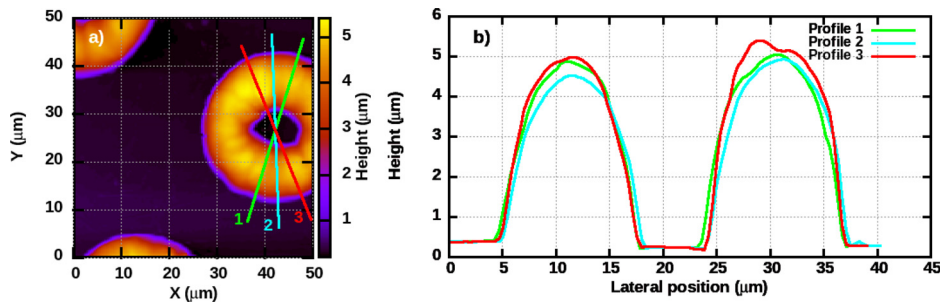


FIG. 3. Height-contrast AFM image (a) of part of array J, and topographical height profiles of a picowell (b) in it. Sections of the picowell where profiles were extracted are indicated on the left panel.

and unirradiated parts was determined. Microhardness of the toruses and the unimplanted regions in array J was measured with a Cypher ES instrument (Asylum Research, Santa Barbara, CA), in which an OMCL-AC160TS cantilever (Olympus Corporation, Japan) was used, with nominal spring constant and resonance frequency of 26 N/m and 300 kHz, respectively. The actual spring constant was measured by using the thermal method by using the procedure built into the driver software of the instrument (AR v.16, based on IgorPro, Wavemetrics, Lake Oswego, OR).

Average picowell dimensions measured in the two AFM experiments were in good agreement. Spatial resolution in both the sample plane and along the normal was below 1 nm in AFM measurements by both Nanosurf Easyscan 2 and Cypher ES.

The results of the microhardness measurements are shown in Fig. 4. The Z-sensor data show the position of the base of the cantilever during indentation (a) and retraction (b). The stiffness, measured from the slope of the indentation curve, of both the background and the torus was about 12 N/m. Considering that the force traces collected in the background (non-irradiated part) and the torus coincide, we may conclude that the ion microbeam irradiation has not altered the microhardness of the ZEONORTM sample.

To demonstrate the applicability of the picowell array to biological measurements, microfluorescence of HeLa Fucci cells was performed. HeLa Fucci cells (RCB2812, RIKEN BRC)⁵⁹ were cultured in Dulbecco's modified Eagle's medium (DMEM, 21885025 Gibco) with 10% fetal bovine serum (Biowest SAS, France), 100 U/ml penicillin, and 100 μ g/ml streptomycin mixture solution (Merck, Germany). Cells were kept in a humidified incubator at 37 °C and 5% CO₂.

The cells were removed from a tissue culture Petri dish using standard trypsinization protocol prior to the experiment. They were washed with 1 ml of Dulbecco's phosphate-buffered saline (DPBS, Corning Inc., Corning, New York, USA) by resuspension and centrifugation at 200 \times g for 5 min and finally resuspended in DPBS solution. The cells were transferred to a Petri dish (627161, Greiner bio-one, Hungary), which was treated with 5% BSA solution for 30 min and then washed and filled with DPBS. The picowell array sample, treated with oxygen plasma, was also stored under the same conditions in a separate Petri dish. Both Petri dishes were scanned with a motorized microscope (Zeiss Axio Observer Z1, Carl Zeiss AG, Oberkochen, Germany) fitted with a digital camera using a 20 \times objective with filter sets 43 HE DsRed and 38 HE EGFP. Fluorescent mode observation was used. For controlled single-cell pickup and subsequent positioning, a computer controlled micropipette system (CellSorter Ltd, Budapest, Hungary) with a micropipette tip of 15 μ m internal diameter (BioMedical Instruments, Zöllnitz, Germany) was employed.^{60–63}

In our experiment, we demonstrated the ability of our fabricated wells to gather and position living cancer cells accurately using a computer-controlled micropipette. ZEONORTM, a hydrophobic material,³⁰ was used in the fabrication of these wells. The cell insertion efficiency was virtually non-existent without plasma treatment, as all attempts failed, and the cells were repelled by the wells. The introduction of plasma treatment remarkably increased the efficiency to 10%, enabling effective deposition of cells within the fabricated structures. The further application of a biological coating like fibronectin could potentially augment this efficiency. We recognize the crucial roles of various factors, including the size of the micropipette opening, its positioning precision, the speed of approach, and the distance between the pipette tip and the targeted well. While these factors certainly influenced the results, their thorough optimization was not the focus of this particular study.

The HeLa Fucci cells were ideal for this experiment due to their continuous expression of color-changing fluorescent protein probes based on their cell cycle state,⁵⁸ easing the process of cell identification. Effective cell insertion was confirmed through fluorescence, with an example illustrated in Fig. 5.

Looking ahead, future studies could explore modifications to the well design, like increasing their depth and size, to potentially improve cell deposition efficiency. Furthermore, a more detailed investigation into optimal micropipette operation could be beneficial, emphasizing not the shortcomings of our study, but the potential advancements to be made in this field.

In summary, a method, namely, direct writing by a high-energy ion microbeam, was proposed for the fabrication of picowell arrays.

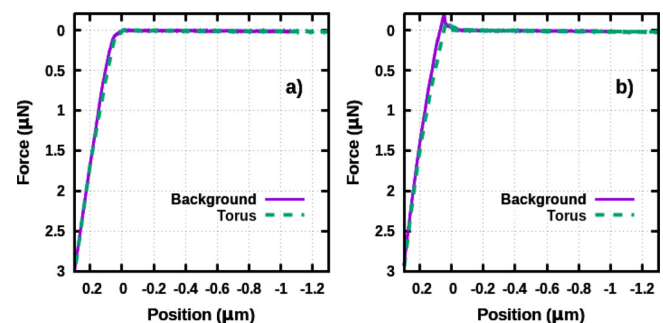


FIG. 4. Microhardness measurements of the picowells of array J. (a) Indentation of the sample surface and the toroidal wall. Continuous line: background, dashed line: torus. (b) Retraction traces for the sample surface and the toroidal wall. Continuous line: background, dashed line: torus.

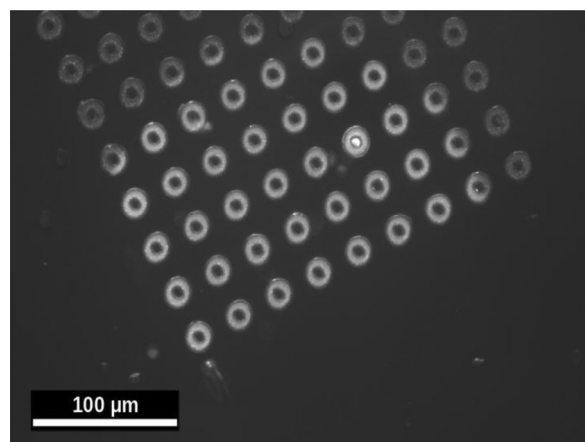


FIG. 5. A Fucci cell emitting strong fluorescent signal is seen in the targeted well. A 43HE DSRED filter was used.

The feasibility of the method was demonstrated by the fabrication of a 9×9 matrix of picowells on Zeonor copolymer. Picowells had an average volume of 820 ± 65 fl. It was proven that the toroidal wall of the ion microbeam implanted picowell had the same microhardness as the unimplanted surface of the sample. Fucci cells were effectively placed in some picowells. They were detected by fluorescence microscopy. By changing the parameters of the fabrication, such as ion species, energy, fluence, and ion microbeam size, reducing picowell volume down to about 100 fl and increasing the volume up to about 50 pl appear feasible. Thus, direct writing of such structures using medium-to-high-energy ion microbeams can compete with direct writing by laser beam. A clear advantage of ion microbeam writing over laser beam writing is the better controllability in depth, allowing for fabrication of three-dimensional structures. Moreover, the recent introduction of ion nanobeam facilities with typical lateral beam sizes in the 200–400 nm range further improve lateral resolution of the ion beam irradiation technique.⁶⁴

Although ion beam accelerators are normally not easily accessible, the proposed method has some clear advantages. First, it is a one-step fabrication. Second, it is a fast method: fabrication of an array can take typically tens of seconds and may take a maximum of a couple of minutes. The method permits a very quick and flexible design of the picowells. Third, besides the polymer used in these experiments, other materials, e.g., glasses, can also be used, although higher fluences (and hence longer irradiation times) may be necessary. Finally, the fabricated surface structures can be also applied as templates for PDMS casting to obtain a negative replica. When a positive replica is needed, the PDMS stamps could be used for UV replication, obtaining by this way the exact copy of the fabricated structures.⁶⁵ Hot embossing using the PDMS stamps into a suitable polymer⁶⁶ is also an option to fabricate the structures in larger quantities in a straightforward manner.

The authors thank Professor G. Orellana Moraleda of the Complutense University of Madrid, Spain, for a helpful discussion and for providing a ZEONOR™ sample for the experiments. Part of this research has been carried out at the CANAM (Centre of Accelerators and Nuclear Analytical Methods) infrastructure LM

2015056. This publication has been supported by OP RDE, MEYS, Czech Republic, under the project CANAM OP, CZ.02.1.01/0.0/0.0/16_013/0001812, and by the Czech Science Foundation (GACR No. 22-10536S). The present work was supported by the Hungarian Academy of Sciences through the Lendület (Momentum) Program, the National Research, Development and Innovation Office (NKFIH) (KKP 129936, PD 134195, K135360, K143321, and TKP2021-EGA-04 Programs). Partial funding from Project VOC-DETECT M-Era-Net project OTKA NNE 131269 was also received.

AUTHOR DECLARATIONS

Conflict of Interest

The authors have no conflicts to disclose.

Author Contributions

Istvan Banyasz: Conceptualization (lead); Data curation (lead); Formal analysis (lead); Investigation (lead); Methodology (equal); Project administration (lead); Supervision (lead); Writing – original draft (lead); Writing – review & editing (lead). **Inna Székács:** Data curation (equal); Formal analysis (equal); Investigation (equal); Methodology (equal); Writing – original draft (equal). **Robert Horváth:** Data curation (equal); Formal analysis (equal); Investigation (equal); Methodology (equal); Writing – original draft (equal). **M. Fried:** Funding acquisition (equal); Writing – original draft (supporting). **Gyula Nagy:** Data curation (equal); Formal analysis (equal); Investigation (equal); Methodology (equal); Writing – original draft (equal); Writing – review & editing (equal). **István Rajta:** Data curation (equal); Investigation (equal); Methodology (equal); Writing – original draft (supporting). **Vladimir Havranek:** Data curation (equal); Investigation (equal); Writing – original draft (supporting). **Anna Macková:** Data curation (equal); Investigation (equal); Writing – original draft (supporting). **Andras J. Laki:** Data curation (equal); Formal analysis (equal); Investigation (equal); Methodology (equal); Writing – original draft (equal). **Miklós S. Z. Kellermayer:** Data curation (equal); Formal analysis (equal); Investigation (equal); Methodology (equal). **Zoltán Sztittner:** Data curation (equal); Formal analysis (equal); Investigation (equal); Methodology (equal); Writing – original draft (equal). **Sandor Kurunczi:** Data curation (equal); Formal analysis (equal); Investigation (equal). **Szabolcs Novák:** Data curation (equal); Formal analysis (equal); Investigation (equal); Methodology (equal); Writing – original draft (equal).

DATA AVAILABILITY

The data that support the findings of this study are available within the article.

REFERENCES

- Q. Zhou, K. Son, Y. Liu, and A. Revzin, *Annu. Rev. Biomed. Eng.* **17**, 165 (2015).
- G. Takatsy, *Kiserl. Orvostud.* **5**, 393 (1950) (in Hungarian).
- S. Lindstrom, M. Eriksson, T. Vazin *et al.*, *PLoS One* **4**, e6997 (2009).
- H. Antypas, M. Veses-Garcia, E. Weibull *et al.*, *Lab Chip* **18**, 1767 (2018).
- D. Bernhard, S. Mall, and P. Pantano, *Anal. Chem.* **73**, 2484 (2001).
- J. R. Rettig and A. Folch, *Anal. Chem.* **77**, 5628 (2005).
- T. Molter, S. McQuaide, M. Suchorolski *et al.*, *Sens. Actuators, B* **135**, 678 (2009).

- ⁸D. Decrop, G. Pardon, and L. Brancato, *ACS Appl. Mater. Interfaces* **9**, 10418 (2017).
- ⁹J. Wöhrle, S. D. Krämer, P. A. Meyer *et al.*, *Sci. Rep.* **10**, 5770 (2020).
- ¹⁰J. Breukers, S. Horta, C. Struyfs *et al.*, *ACS Appl. Mater. Interfaces* **13**, 2316 (2021).
- ¹¹Vittrion, see <https://www.vittrion.com/en/products/high-definition-picowells/> for “LIDE PicoWells,” accessed 30 August 2022.
- ¹²W. Liu, Z. Li, Y. Liu *et al.*, *RSC Adv.* **9**, 2865 (2019).
- ¹³D. K. Wood, D. M. Weingeist, S. N. Bhatia, and B. P. Engelward, *Proc. Natl. Acad. Sci.* **107**, 10008 (2010).
- ¹⁴T. P. Aicher, S. Carroll, G. Raddi *et al.*, “Seq-Well: A sample-efficient, portable picowell platform for massively parallel single-cell RNA sequencing,” in *Single Cell Methods. Methods in Molecular Biology*, edited by V. Proserpio (Humana, New York, 2019), Vol. 1979.
- ¹⁵Q. M. Han, E. Bradshaw, B. Nilsson *et al.*, *Lab Chip* **10**, 1391 (2010).
- ¹⁶J. R. Choi, J. H. Lee, A. Xu *et al.*, *Lab Chip* **20**, 4539–4551 (2020).
- ¹⁷A. O. Ogunniyi, C. M. Story, E. Papa *et al.*, *Nat. Protoc.* **4**, 767 (2009).
- ¹⁸S. Park, J. Han, W. Kim *et al.*, *J. Biotechnol.* **156**, 197 (2011).
- ¹⁹A. J. Torres, A. S. Hill, and J. C. Love, *Anal. Chem.* **86**, 11562 (2014).
- ²⁰J. Woo, S. M. Williams, L. M. Markillie *et al.*, *Nat. Commun.* **12**, 6246 (2021).
- ²¹Y. Seo, S. Jeong, J. K. Lee *et al.*, *Nano Converg.* **5**, 9 (2018).
- ²²J. Y. Shin, J. Y. Park, C. Liu *et al.*, *Pure Appl. Chem.* **77**, 801 (2005).
- ²³W. D. Niles and P. J. Coassin, *ASSAY Drug Dev. Technol.* **6**, 577 (2008).
- ²⁴P. Ray and A. J. Steckl, *ACS Sens.* **4**, 1346 (2019).
- ²⁵A. Agha, W. Waheed, N. Alamoodi *et al.*, *Macromol. Mater. Eng.* **307**, 2200053 (2022).
- ²⁶T. G. Henares, F. Mizutani, and H. Hisamoto, *Anal. Chim. Acta* **611**, 17 (2008).
- ²⁷D. Brassard, L. Clime, K. Li *et al.*, *Lab Chip* **11**, 4099 (2011).
- ²⁸Y. Qi, Y. Wang, C. Zhao *et al.*, *ACS Appl. Mater. Interfaces* **11**, 28690 (2019).
- ²⁹C. Volcke, R. P. Gandhiraman, V. Gubala *et al.*, *Biosens. Bioelectron.* **25**, 1875 (2010).
- ³⁰P. S. Nunes, P. D. Ohlsson, O. Ordeig, and J. P. Kutter, *Microfluid. Nanofluid.* **9**, 145 (2010).
- ³¹J. Prada, C. Cordes, C. Harms, and W. Lang, *Sensors* **19**, 1178 (2019).
- ³²S. Laib and B. D. MacCraith, *Anal. Chem.* **79**, 6264 (2007).
- ³³R. P. Gandhiraman, C. Volcke, V. Gubala *et al.*, *J. Mater. Chem.* **20**, 4116 (2010).
- ³⁴R. P. Gandhiraman, V. Gubala, L. C. H. Nam *et al.*, *Colloids Surf., B* **79**, 270 (2010).
- ³⁵W. F. X. Frank, A. Schosser, A. Stelmaszyk, and J. Schulz, *Proc. SPIE* **10285**, 1028505 (1996).
- ³⁶T. C. Sum, A. A. Bettiol, H. L. Seng *et al.*, *Nucl. Inst. Methods Phys. Res. Sect. B* **210**, 266 (2003).
- ³⁷I. Rajta, M. Chatzichristidi, E. Baradacs *et al.*, *Nucl. Inst. Methods Phys. Res. Sect. B* **260**, 414 (2007).
- ³⁸R. Huszank, S. Z. Szilasi, K. Vad, and I. Rajta, *Nucl. Inst. Methods Phys. Res. Sect. B* **267**, 2299 (2009).
- ³⁹S. Z. Szilasi, J. Kokavec, R. Huszank, and I. Rajta, *Appl. Surf. Sci.* **257**, 4612 (2011).
- ⁴⁰G. U. L. Nagy, V. Lavrentiev, I. Banyasz *et al.*, *Thin Solid Films* **636**, 634 (2017).
- ⁴¹S. Z. Szilasi, J. Budai, Z. Papa *et al.*, *Mater. Chem. Phys.* **131**, 370 (2011).
- ⁴²M. Varasane, I. Bogdanovic-Radovic, Z. Pastuovic, and M. Jaksic, *Nucl. Inst. Methods Phys. Res. Sect. B* **269**, 2413 (2011).
- ⁴³G. U. L. Nagy, R. Kerékgyarto, A. Csik *et al.*, *Nucl. Inst. Methods Phys. Res. Sect. B* **449**, 71 (2019).
- ⁴⁴O. Romanenko, V. Havránek, P. Malinsky *et al.*, *Nucl. Inst. Methods Phys. Res. Sect. B* **461**, 175 (2019).
- ⁴⁵J. Jiang, N. Qin, and T. H. Tao, *J. Micromech. Microeng.* **30**, 033001 (2020).
- ⁴⁶G. U. L. Nagy, Z. Szoboszlai, and I. Rajta, *Acta Phys. Pol., A* **136**, 250 (2019).
- ⁴⁷P. Mela, A. van den Berg, Y. Fintschenko *et al.*, *Electrophoresis* **26**, 1792 (2005).
- ⁴⁸Zeon, see <https://www.zeon.co.jp/en/business/enterprise/resin/cop/> for “ZEONOR.”
- ⁴⁹F. Watt, A. A. Bettiol, J. A. van Kan *et al.*, *Int. J. Nanosci.* **4**, 269 (2005).
- ⁵⁰P. Malinský, O. Romanenko, V. Havranek *et al.*, *Surf. Interface Anal.* **52**, 1171 (2020).
- ⁵¹O. Romanenko, P. Slepicka, P. Malinsky *et al.*, *Surf. Interface Anal.* **52**, 1040 (2020).
- ⁵²P. Malinsky, A. Romanenko, V. Havranek *et al.*, *Appl. Surf. Sci.* **528**, 146802 (2020).
- ⁵³M. Cutroneo, V. Havranek, A. Mackova *et al.*, *Radiat. Eff. Defects Solids* **175**, 307 (2020).
- ⁵⁴O. Romanenko, V. Havranek, A. Mackova *et al.*, *Rev. Sci. Instrum.* **90**(9), 099901 (2019).
- ⁵⁵J. F. Ziegler, M. D. Ziegler, and J. P. Biersack, *Nucl. Inst. Methods Phys. Res. Sect. B* **268**, 1818 (2010).
- ⁵⁶R. S. Thomaz and R. M. Papaleo, “Ion beam modification of poly (methyl methacrylate) (PMMA),” in *Radiation Effects in Polymeric Materials*, Springer Series on Polymer and Composite Materials, edited by V. Kumar, B. Chaudhary, V. Sharma, and K. Verma (Springer, Cham, 2019).
- ⁵⁷I. P. Jain and G. Agarwal, *Surf. Sci. Rep.* **66**, 77–172 (2011).
- ⁵⁸H. Beyer, *J. R. Microsc. Soc.* **87**, 171 (1967).
- ⁵⁹A. Sakaue-Sawano, H. Kurokawa, T. Morimura *et al.*, *Cell* **132**, 487 (2008).
- ⁶⁰T. Gerecsei, I. Erdődi, B. Peter *et al.*, *J. Colloid Interface Sci.* **555**, 245–253 (2019).
- ⁶¹R. Salánki, C. Hős, N. Orgovan *et al.*, *PLoS One* **9**(10), e111450 (2014).
- ⁶²R. Ungai-Salánki, E. Haty, T. Gerecsei *et al.*, *Sci. Rep.* **11**, 18500 (2021).
- ⁶³B. Francz, R. Ungai-Salánki, É. Sautner *et al.*, *Microfluid. Nanofluid.* **24**, 12 (2020).
- ⁶⁴I. Rajta, G. U. L. Nagy, I. Vajda *et al.*, *Nucl. Inst. Methods Phys. Res. Sect. B* **449**, 94 (2019).
- ⁶⁵R. Horvath, L. R. Lindvold, and N. B. Larsen, *J. Micromech. Microeng.* **13**, 419 (2003).
- ⁶⁶R. Horvath, H. C. Pedersen, N. Skivesen *et al.*, *J. Micromech. Microeng.* **15**, 1260 (2005).